Yersinia pestis Subverts the Dermal Neutrophil Response in a Mouse Model of Bubonic Plague

Jeffrey G. Shannon,[a] Aaron M. Hasenkrug,[a] David W. Dorward,[b] Vinod Nair,[b] Aaron B. Carmody,[b] B. Joseph Hinnebusch[a]

Laboratory of Zoonotic Pathogens,[a] Research Technologies Branch,[b] Rocky Mountain Laboratories, National Institute of Allergy and Infectious Diseases, National Institutes of Health, Hamilton, Montana, USA

ABSTRACT **The majority of human *Yersinia pestis* infections result from introduction of bacteria into the skin by the bite of an infected flea. Once in the dermis, *Y. pestis* can evade the host's innate immune response and subsequently disseminate to the draining lymph node (dLN). There, the pathogen replicates to large numbers, causing the pathognomonic bubo of bubonic plague. In this study, several cytometric and microscopic techniques were used to characterize the early host response to intradermal (i.d.) *Y. pestis* infection. Mice were infected i.d. with fully virulent or attenuated strains of dsRed-expressing *Y. pestis*, and tissues were analyzed by flow cytometry. By 4 h postinfection, there were large numbers of neutrophils in the infected dermis and the majority of cell-associated bacteria were associated with neutrophils. We observed a significant effect of the virulence plasmid (pCD1) on bacterial survival and neutrophil activation in the dermis. Intravital microscopy of i.d. *Y. pestis* infection revealed dynamic interactions between recruited neutrophils and bacteria. In contrast, very few bacteria interacted with dendritic cells (DCs), indicating that this cell type may not play a major role early in *Y. pestis* infection. Experiments using neutrophil depletion and a CCR7 knockout mouse suggest that dissemination of *Y. pestis* from the dermis to the dLN is not dependent on neutrophils or DCs. Taken together, the results of this study show a very rapid, robust neutrophil response to *Y. pestis* in the dermis and that the virulence plasmid pCD1 is important for the evasion of this response.**

IMPORTANCE ***Yersinia pestis* remains a public health concern today because of sporadic plague outbreaks that occur throughout the world and the potential for its illegitimate use as a bioterrorism weapon. Since bubonic plague pathogenesis is initiated by the introduction of *Y. pestis* into the skin, we sought to characterize the response of the host's innate immune cells to bacteria early after intradermal infection. We found that neutrophils, innate immune cells that engulf and destroy microbes, are rapidly recruited to the injection site, irrespective of strain virulence, indicating that *Y. pestis* is unable to subvert neutrophil recruitment to the site of infection. However, we saw a decreased activation of neutrophils that were associated with *Y. pestis* strains harboring the pCD1 plasmid, which is essential for virulence. These findings indicate a role for pCD1-encoded factors in suppressing the activation/stimulation of these cells *in vivo*.**

Received 11 March 2013 **Accepted** 26 July 2013 **Published** 27 August 2013

Citation Shannon JG, Hasenkrug AM, Dorward DW, Nair V, Carmody AB, Hinnebusch BJ. 2013. *Yersinia pestis* subverts the dermal neutrophil response in a mouse model of bubonic plague. mBio 4(5):e00170-13. doi:10.1128/mBio.00170-13.

Editor Olaf Schneewind, The University of Chicago

Address correspondence to Jeffrey G. Shannon, jshannon@niaid.nih.gov.

Yersinia pestis is a Gram-negative bacterial pathogen that can cause three distinct forms of plague: pneumonic, septicemic, and bubonic. Bubonic plague is the most common form in humans and results from the introduction of *Y. pestis* into the skin by the bite of an infected flea. Once in the dermis, *Y. pestis* can survive, replicate, and eventually migrate to the regional draining lymph node (dLN). There, the pathogen can replicate to very high numbers, resulting in massive swelling of the lymph node, termed a bubo. The cellular architecture of this bubo can subsequently break down, resulting in systemic hematogenous spread of the bacteria.

The progression of *Y. pestis* infection can be divided into two distinct phases. The initial bubonic phase, consisting of the first 2 to 3 days postinfection, is characterized by a minimal inflammatory response in the dLN despite the presence of large numbers of replicating bacteria (1, 2). If the infection is allowed to spread beyond the regional draining lymphoid tissue, the proinflammatory or hyperinflammatory phase of infection ensues. This secondary septic phase is characterized by a massive upregulation of myriad inflammatory cytokines that quickly leads to multiorgan system failure and the death of the infected individual (1, 2).

Current understanding of the interactions between *Y. pestis* and mammalian host cells *in vivo* is limited to just a few published studies. Virulent *Y. pestis* associates with polymorphonuclear leukocytes (neutrophils) and macrophages (Mφ) after subcutaneous infection (3). It is thought that bacteria are quickly killed after phagocytosis by neutrophils, whereas *Y. pestis* bacteria taken up by Mφ are able to survive, replicate, and disseminate (4). This hypothesis is supported by a number of *in vitro* studies; however, the roles of these cell types in the innate response to *Y. pestis in vivo* remain unclear.

Virulent strains of *Y. pestis* possess a 70-kb virulence plasmid

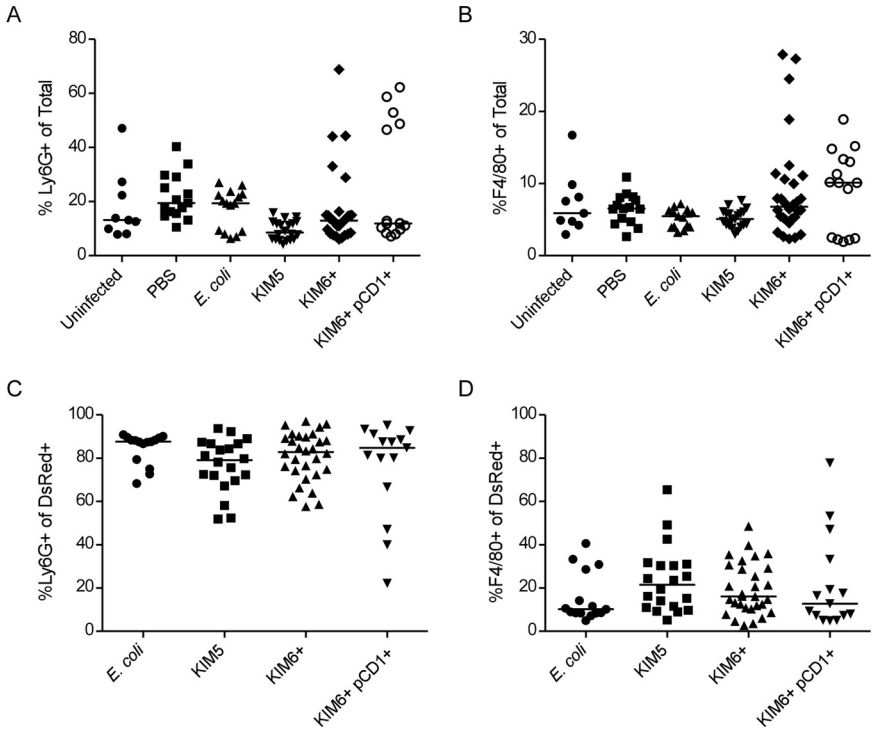

FIG 1 *Y. pestis* associates with neutrophils recruited to the site of infection. Single-cell suspensions of mouse ear dermis were analyzed by flow cytometry after they were injected with PBS, *E. coli*, KIM5/pCD1$^+$, KIM6$^+$ *pgm*$^+$, or KIM6$^+$/pCD1$^+$ (WT) or left uninjected. Total number of neutrophils (A) or Mφ (B) in the ear dermis cell preparations at 4 hpi were determined by flow cytometry. Results are expressed as percentages of the total number of events that were either Ly6G$^+$ or F4/80$^+$, respectively. The percentage of dsRed$^+$ events that were also Ly6G$^+$ (C) or F4/80$^+$ (D) indicates the percentage of bacterium-associated cells that were neutrophils or Mφ, respectively. Each symbol represents one mouse, and the line indicates the median. The results shown are the pooled data from a minimum of three separate experiments.

(pCD1) that encodes a type III secretion apparatus and several type III secreted effectors. These effectors dramatically affect a variety of cell signaling pathways in the mammalian host, resulting in the inhibition of both innate and adaptive immune responses (5). The pCD1 plasmid is required for the immune suppression observed early after *Y. pestis* infection (1). Additionally, the *Y. pestis* genome contains a pathogenicity island termed the pigmentation locus (*pgm*). This locus contains genes involved in a variety of functions necessary for flea colonization and transmission, iron acquisition, and intracellular survival (6–8).

The goals of this study were to characterize the very early host cell response to intradermal (i.d.) *Y. pestis* and to evaluate the effects of pCD1 and *pgm* on this response. To this end, we used flow cytometry and intravital microscopy to study a mouse i.d. model of bubonic plague. Additionally, we examined the effects of neutrophil and dendritic cell (DC) migration on the kinetics of *Y. pestis* dissemination. Our results indicate a prominent role for neutrophils in the very early response to plague bacilli in the dermis and show that the virulence plasmid pCD1 is important for evasion of this rapid response.

RESULTS

***Y. pestis* associates predominantly with neutrophils early after i.d. infection.** We used a mouse model of bubonic plague to determine which host cell types are recruited to the dermis early after *Y. pestis* infection. Mice were injected i.d. in the ear with 1×10^5 CFU of a fully virulent *Y. pestis* strain, KIM6$^+$/pCD1$^+$ (wild type [WT]); attenuated strain KIM6$^+$/pCD1$^-$ *pgm*$^+$, which lacks the virulence plasmid; or attenuated strain KIM5/pCD1$^+$ *pgm*, which possesses the virulence plasmid but lacks the pigmentation locus (*pgm*) required for virulence by the i.d. or subcutaneous route of infection (9). Additionally, groups of mice were injected i.d. with a nonpathogenic strain of *E. coli* or phosphate-buffered saline (PBS) for comparison of the host response to innocuous bacteria or the injection itself. All of the bacterial strains possessed the pTAC-dsRed plasmid, and dsRed expression was induced with isopropyl-β-D-thiogalactopyranoside (IPTG) prior to infection. The inoculum of 1×10^5 is at least 2 orders of magnitude more than what an infected flea usually transmits (10); however, we found this dose necessary for reliable and reproducible visualization of dsRed$^+$ populations by flow cytometry (data not shown). A representative example of the gating strategy used to exclude background autofluorescence from our dsRed$^+$ populations is shown in Fig. S1A in the supplemental material.

At 4 h postinfection (hpi), mice were euthanized and single-cell suspensions of ear dermis were stained with a panel of fluorescently labeled antibodies (Abs) specific for mouse Mφ, neutrophil, B cell, and DC surface markers and analyzed by flow cytometry. We observed an increase in the proportion of neutrophils in some of the KIM6$^+$- and KIM6$^+$/pCD1-infected mice; however, the results were quite variable. Overall, neutrophils made up 5 to 10% of the total number of cells from the ears of most of the animals (Fig. 1A; see Fig. S1B in the supplemental material). We did not see a significant increase in the Mφ proportion in the ear at this early time point (Fig. 1B; see Fig. S1C). B cells

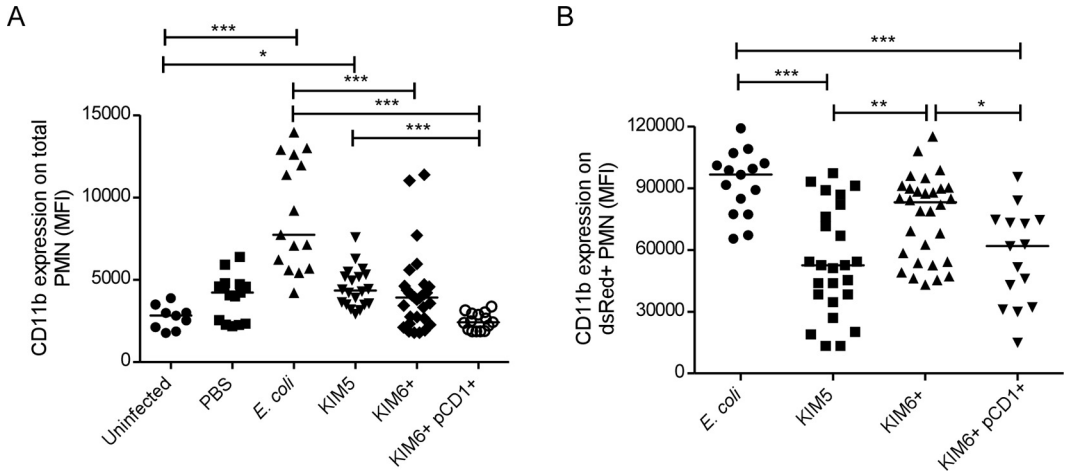

FIG 2 *Y. pestis* inhibits neutrophil activation via a pCD1-dependent mechanism. Single-cell suspensions of mouse ear dermis were analyzed by flow cytometry after they were injected with PBS, *E. coli*, KIM5/pCD1$^+$, KIM6$^+$ *pgm*$^+$, or KIM6$^+$/pCD1$^+$ (WT) or left uninjected. The activation state of the total neutrophil population (Ly6G$^+$) (A) in the ear dermis or the neutrophils that were associated with bacteria (Ly6G$^+$ dsRed$^+$) (B) at 4 hpi was determined as the CD11b expression level on the cell surface as measured by flow cytometry. Each symbol represents one mouse, and the line indicates the median. The results shown are the pooled data from a minimum of three separate experiments. *, $P < 0.05$; **, $P < 0.01$; ***, $P < 0.001$. PMN, polymorphonuclear leukocytes; MFI, mean fluorescence intensity.

and DCs were present in much lower numbers than Mφ and neutrophils and did not increase over the levels found in uninfected ears (data not shown).

Injection of bacteria expressing the fluorescent protein dsRed allowed us to identify the host cell types the bacteria were associating with in the dermis. At 4 hpi, we observed that >80% of the dsRed$^+$ events in the dermal cell suspensions were also positive for the neutrophil specific marker Ly6G (Fig. 1C). Most of the dsRed$^+$ Ly6G$^-$ events were F4/80$^+$, indicating that a large proportion of the remaining bacteria were associated with Mφ (Fig. 1D). A small percentage of events were dsRed$^+$ Ly6G$^+$ F4/80$^+$ (data not shown). This may indicate some interaction between Mφ and neutrophils in the dermis but could also be an artifact of the cell isolation and staining procedure

Taken together, these data indicate that neutrophils may be the predominant innate immune cell type encountered by *Y. pestis* very early during the establishment of bubonic plague.

***Y. pestis* strains possessing the virulence plasmid pCD1 inhibit neutrophil activation *in vivo*.** Neutrophils undergo an activation process after contact with a variety of inflammatory stimuli. CD11b is a β2 integrin that, together with CD18, forms complement receptor 3, a molecule essential for extravasation of neutrophils (11). Recognition of molecules such as bacterial lipopolysaccharide (LPS) or formylated peptides, tumor necrosis factor, complement component C5a, and leukotriene B_4 by their cognate receptors on neutrophils results in mobilization of CD11b from intracellular stores to the cell surface (12). We determined the activation state of the dermal neutrophil population by measuring CD11b expression levels on the surface of Ly6G$^+$ cells. Analysis of the total population of neutrophils showed that infection with the fully virulent KIM6$^+$/pCD1$^+$ (WT) strain resulted in no measurable upregulation of CD11b expression, suggesting a lack of neutrophil activation in the infected ear (Fig. 2A). In contrast, the attenuated KIM5/pCD1$^+$ strain caused an increase in total neutrophil CD11b$^+$ expression compared to the uninfected control but not the PBS-injected ear (Fig. 2A). Infection with the KIM6$^+$ *pgm*$^+$ strain did not result in significantly increased neutrophil activation; however, the results of these experiments were quite variable. The levels of activation seen in response to any of the *Y. pestis* strains were consistently lower than those observed after infection with avirulent *E. coli*. Interestingly, when gating was narrowed to dsRed$^+$ events, thereby focusing only on cells that were associated with bacteria, we saw significantly less neutrophil activation after infection with both of the pCD1-possessing strains, KIM5/pCD1$^+$ and KIM6$^+$/pCD1$^+$, than after infection with KIM6$^+$ (Fig. 2B). Thus, the fully virulent strain of *Y. pestis* appears to subvert the normal activation process of all neutrophils recruited to the site of infection, whereas only the neutrophils that directly associated with KIM5 showed lower levels of activation.

To follow up on these *in vivo* results, we examined the effects of *Y. pestis* infection on mouse neutrophils *in vitro*. Bone marrow cells from four different mice were infected with KIM5/pCD1$^+$ or KIM6$^+$ *pgm*$^+$ for 4 h. The cells were then stained for the neutrophil marker Ly6G, and activation of these cells was determined by measurement of CD11b expression levels (Fig. 3). The data from this *in vitro* experiment support the conclusion that *Y. pestis* can inhibit neutrophil activation by a pCD1-dependent mechanism.

Presence of pCD1 affects *Y. pestis* viability at 4 hpi. During preparation of the ear dermis cell suspension for flow cytometry staining, the samples are subjected to multiple low-speed centrifugations (500 × *g*), resulting in the elimination of >95% of the non-cell-associated bacteria from the final cell pellet (data not shown). We took advantage of this differential centrifugation as a way of quantifying the total number of cell-associated CFU in the ear dermis samples. We compared the total number of CFU in the initial, prespin dermal cell suspension to the number of CFU present in the cell pellet after three centrifugations and washes. The results show a trend toward lower cell association of pCD1$^+$ strains than of KIM6$^+$, but this difference was not statistically significant (Fig. 4A). However, when we looked at the total CFU count recovered from the ear as a percentage of the CFU count in the inoculum, we saw a reduction in the CFU numbers of the

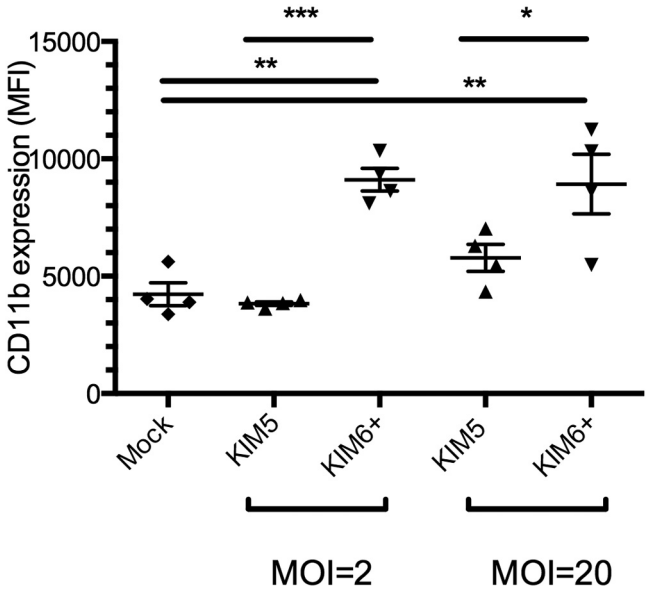

FIG 3 In vitro confirmation that *Y. pestis* inhibits murine neutrophil activation via a pCD1-dependent mechanism. The activation state of neutrophils from mouse bone marrow was determined after mock infection or infection with KIM5 or KIM6$^+$ at an MOI of 2 or 20 *in vitro*. Flow cytometry was used to determine the CD11b expression level on the surface of Ly6G$^+$ cells (neutrophils) at 4 hpi. Cells from four C57BL/6 mice were analyzed. Each symbol represents one mouse, and the line indicates the median with the range. The results shown are from one experiment and are representative of three independent experiments. *, $P < 0.05$; **, $P < 0.01$; ***, $P < 0.001$. MFI, mean fluorescence intensity.

KIM6$^+$ strain present at 4 hpi, whereas the pCD1$^+$ strains had increased in number (Fig. 4B).

These data show that survival of these bacteria in the dermis is compromised even at this very early time point, and although the differences were not significant, the pCD1$^-$ strain may associate with host cells to a greater extent. However, it is important to note that interpretation of the CFU cell association data is complicated by the reduced survival/replication of the pCD1$^-$ strain *in vivo*. In contrast, pCD1 possessing strains, even the attenuated KIM5 strain, show an increase in bacterial numbers and a trend toward reduced cell association at 4 hpi. Additionally, when we look at both the CFU data in Fig. 4B and the neutrophil activation data in Fig. 2, it is interesting that there is decreased neutrophil activation after infection with the fully virulent KIM6$^+$/pYV$^+$ strain despite the presence of 5- to 10-fold more CFU in the mouse ear than of KIM6$^+$/pCD1$^-$ CFU.

Intravital microscopy reveals a robust neutrophil response to i.d. *Y. pestis*. The flow cytometry data showing the large numbers of neutrophils present in *Y. pestis*-infected dermis and the observation that the vast majority of cell-associated bacteria were associated with neutrophils led us to examine the bacterium-neutrophil interactions in the dermis more thoroughly. To accomplish this, we used an intravital confocal microscopy technique to image transgenic mice that express high levels of enhanced green fluorescent protein (eGFP) in neutrophils (LysM-eGFP mice) and, to a lesser extent, in cells of the monocyte lineage (13, 14). LysM-eGFP mice were infected i.d. in the ear with 1×10^3 dsRed-expressing bacteria and imaged from ~15 min postinfection to >4 hpi. Because of a lack of suitable microscopy equipment in our biosafety level 3 (BSL-3) laboratory, we were limited to using only the attenuated KIM5 and KIM6$^+$ strains of *Y. pestis* and avirulent *E. coli* for these studies.

A rapid influx of eGFP^{bright} neutrophils was seen after injection of the KIM6$^+$ *pgm*$^+$ strain (Fig. 5A; see Movie S1 in the supplemental material). Most of the bacteria remained motionless until they associated with an eGFP^{bright} cell. After association, many of the bacteria appeared to comigrate out of the field of view with eGFP^{bright} cells. The neutrophil influx occurred rapidly after infection, with the first cells arriving at the injection site within the first 30 min postinfection. By 2 hpi, the neutrophils in the field of view were too numerous to count and distinct association of a subset of bacteria with neutrophils was observed. In Movie S1R, the green channel has been turned off to allow better visualization of the red bacteria. At 4 hpi, there were still bacteria that remained stationary and apparently had not interacted with neutrophils.

Time-lapse images of the LysM-eGFP mice after infection with the pCD1-possessing KIM5 strain yielded similar results (Fig. 5B; see Movie S2 in the supplemental material). Again we saw a rapid

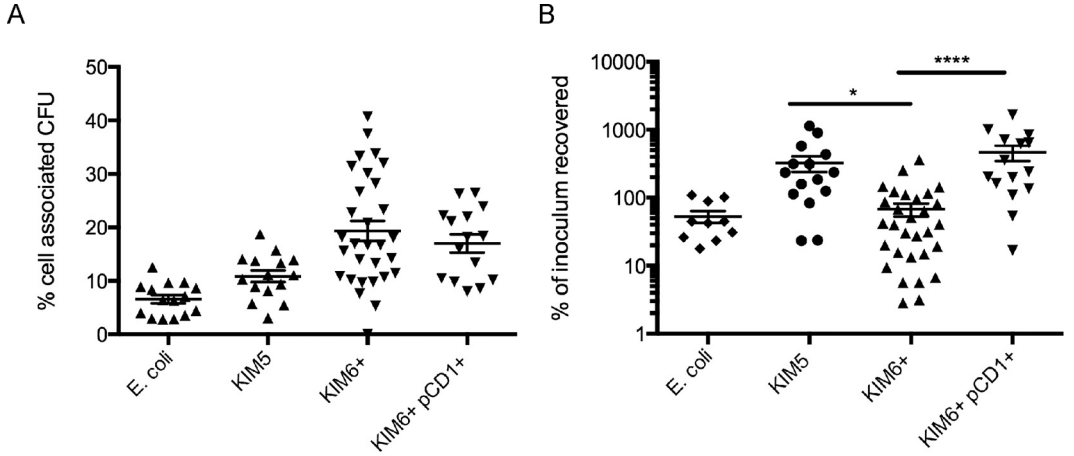

FIG 4 Reduced recovery of viable pCD1$^-$ *Y. pestis* from the ear dermis. (A) The number of bacterial CFU that were cell associated is shown as a percentage of the total number of CFU recovered from the ear at 4 hpi. (B) The total number of viable bacteria present in the ear dermis at 4 hpi is shown as a percentage of the actual inoculum. The results shown are pooled data from a minimum of three separate experiments. *, $P < 0.05$; ****, $P < 0.0001$.

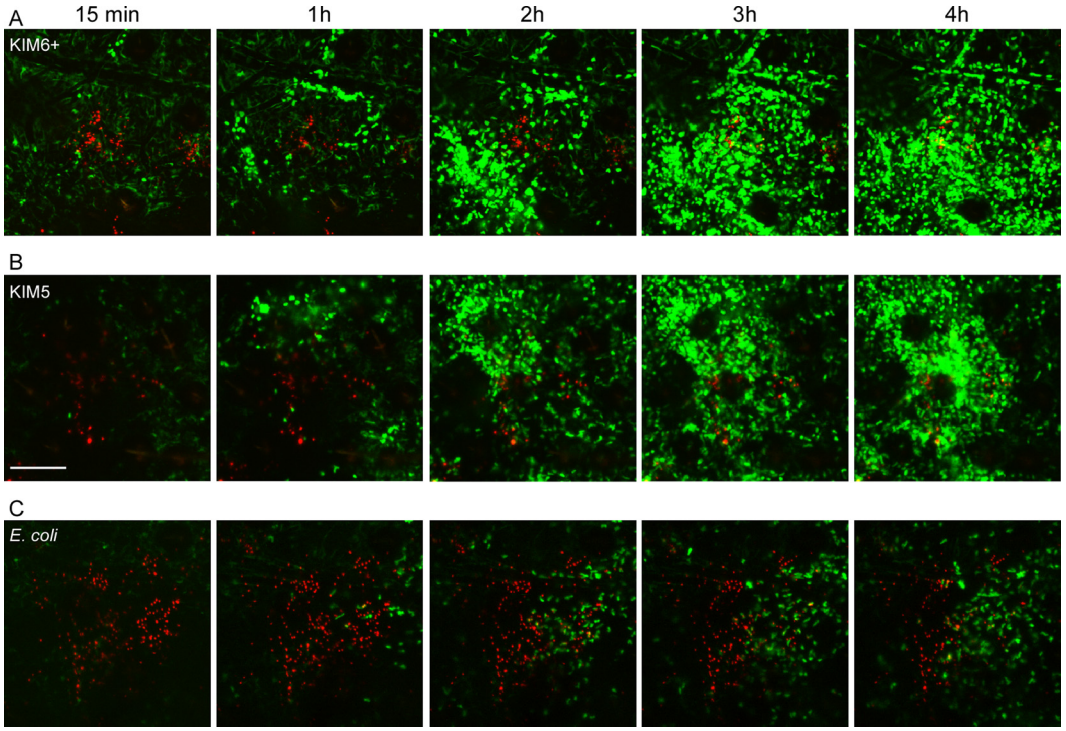

FIG 5 Intravital microscopy shows rapid recruitment of neutrophils to the site of infection. LysM-eGFP mice were injected i.d. in the ear with ~1 × 10^3 KIM6$^+$/pTac-dsRed (A), KIM5/pTac-dsRed (B), or *E. coli*/pTac-dsRed (C) and imaged by confocal microscopy from approximately 15 min postinfection to >4 hpi. z-stacks 40 to 50 μm deep were captured at 2-min intervals for the duration of each experiment. A montage of compressed z-stacks of individual frames at 15 min postinfection and 1, 2, 3, and 4 hpi is shown for each experiment. Neutrophils are bright green, and bacteria are red. Each time series is from one experiment and representative of a minimum of three independent experiments. The scale bar represents 70 μm.

neutrophil influx and eventual association of neutrophils with some of the dsRed-expressing bacteria. Similar to what was seen with KIM6$^+$, the neutrophils formed large aggregates at the injection site. A number of bacteria appeared to comigrate with the eGFP^{bright} neutrophils out of the field of view. As with the KIM6$^+$ strain, at 4 hpi, there were a small proportion of bacteria that had not moved or associated with a neutrophil or other eGFP$^+$ cell. The bacterial movement can be seen more clearly in Movie S2R, where the green channel has been removed.

When an avirulent *E. coli* strain was injected, we observed qualitative differences between the neutrophil response to this innocuous bacterium and the *Y. pestis* strains (Fig. 5C; see Movie S3 in the supplemental material). There was a rapid neutrophil influx, and the neutrophil-bacterium association appeared to occur much more quickly than that seen with *Y. pestis*. By 4 hpi, most of the dsRed$^+$ *E. coli* that had colocalized with neutrophils had migrated out of the field of view (Movie S3R shows the dsRed$^+$ bacteria without the green channel). Furthermore, we did not see the large aggregates of neutrophils that were seen in response to *Y. pestis*. The majority of neutrophils continue to move after association with the bacteria.

Neutrophil-associated *Y. pestis* bacteria are predominantly intracellular. The flow cytometry and intravital microscopy experiments described above showed apparent close association of *Y. pestis* with neutrophils *in vivo*. To determine if these bacteria were adhering to the outside of cells or if they had been phagocytosed, we prepared cytospin slides of ear dermis single-cell suspensions at 4 hpi from mice infected with dsRed$^+$ bacteria. The slides were then fluorescently stained for Ly6G$^+$ cells and nuclei and imaged by confocal microscopy. In agreement with the flow cytometry data (Fig. 1D), >80% of the cells that contained dsRed$^+$ bacteria also stained with the anti-Ly6G Ab (green) and displayed multilobed nuclei, indicating that they were neutrophils (Fig. 6). Cross-section views of z-stacks revealed that >95% of the neutrophil-associated bacteria were completely surrounded by Ly6G staining, suggesting that they were intracellular (Fig. 6). Comparable results were obtained with the KIM6$^+$ *pgm*$^+$ and

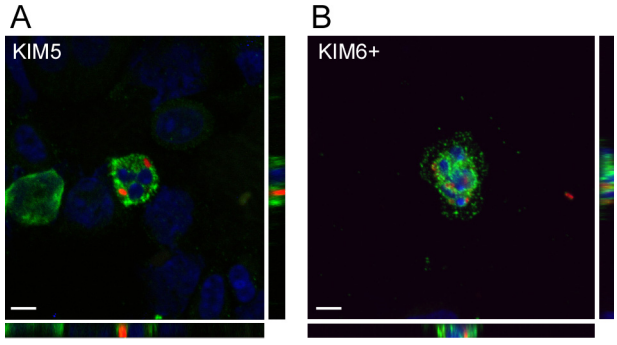

FIG 6 Confocal microscopy of dermal cell cytospin preparations confirms the association of *Y. pestis* with neutrophils. Mice were infected i.d. in the ear with 1 × 10^5 dsRed-expressing KIM5 (A) or KIM6$^+$ (B) bacteria (red), and dermal cell suspensions were prepared at 4 hpi. Cytospins of the ear cell suspensions were fixed and stained for Ly6G (green) and DAPI (blue), and z-stack images were generated by confocal microscopy. The scale bars represent 5 μm.

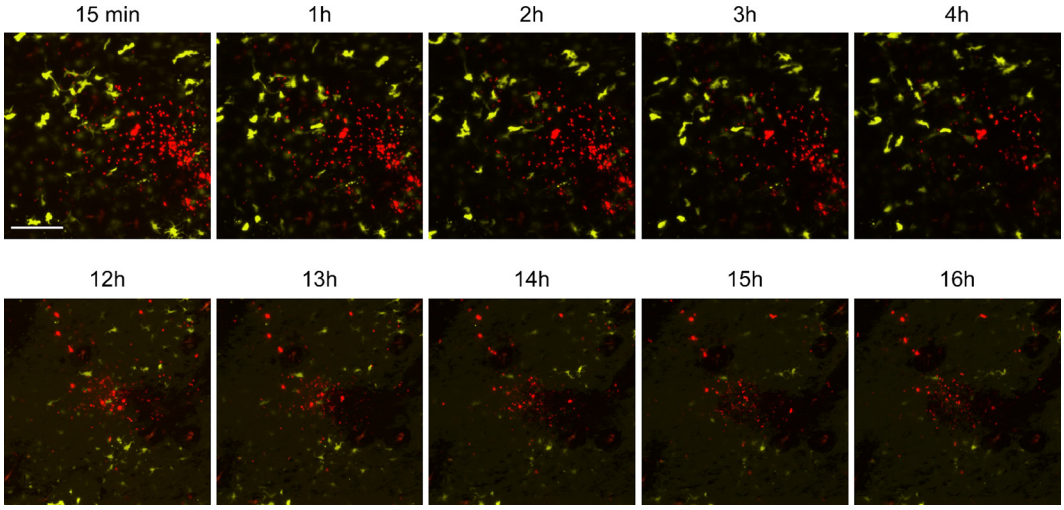

FIG 7 Intravital microscopy reveals minimal interaction between *Y. pestis* and CD11c$^+$ cells in the dermis. CD11c-YFP mice were injected i.d. in the ear with KIM6$^+$/pTac-dsRed and imaged from 15 min postinfection to 4.5 hpi or from 12 to >16 hpi by confocal microscopy. z-stacks 40 to 50 μm deep were captured at 2-min intervals for the duration of each experiment. A montage of compressed z-stacks from individual frames at 15 min postinfection and 1, 2, 3, and 4 hpi (top row) or 12, 13, 14, 15, and 16 hpi (bottom row) are shown for each experiment. Each time series is from one experiment and representative of a minimum of three independent experiments. The scale bar represents 70 μm.

KIM5/pCD1$^+$ strains of *Y. pestis*. Between 10 and 20% of the dsRed$^+$ bacteria were associated with Ly6G$^-$ cells (data not shown). The identity of these cells is unknown, but on the basis of their morphology and the flow cytometry data shown in Fig. 1E, they are likely Mφ.

There is minimal interaction between *Y. pestis* and CD11c$^+$ cells in the dermis. *Y. pestis* is a nonmotile bacterial pathogen that migrates from the dermis to the regional dLN in bubonic plague. DCs are antigen-presenting cells that reside in peripheral tissues such as the dermis, where they engulf antigens and ferry them to lymphoid tissue to initiate an adaptive immune response. Because of this DC-to-dLN traffic, many have speculated that DCs play a role in the dissemination of *Y. pestis* from the dermis to the dLN. We observed by flow cytometry that the number of DCs in the dermis is very low compared to the number of neutrophils recruited to the tissue at 4 hpi and that there are very few dsRed$^+$ DCs in the infected dermis (data not shown). Furthermore, intravital microscopy showed very little movement of bacteria that did not interact with eGFP^{bright} neutrophils. However, we decided to examine potential *Y. pestis*-DC interactions in the dermis more closely by using intravital microscopy.

To image DCs *in vivo*, we used a transgenic mouse strain that expresses yellow fluorescent protein (YFP) under the control of the mouse integrin alpha X (*itgaX*) promoter, resulting in YFP expression in CD11c$^+$ DCs (15). When we imaged a mouse from ~15 min postinfection to >4 hpi with KIM6$^+$, we observed very little association of YFP$^+$ cells with dsRed$^+$ bacteria (Fig. 7; see Movie S4 in the supplemental material). We observed two distinct clusters of red bacteria that appeared to comigrate with motile YFP$^+$ cells early after infection (depicted by arrows in Movie S4), but this phenomenon was rare. By 4 hpi, a large number of bacteria were moving and the majority of this movement appeared to be independent of YFP$^+$ cells. To determine if more interaction of *Y. pestis* with DCs occurred at later time points, we imaged an infected mouse from 12 to 16 hpi. In these experiments, there was dynamic movement of bacteria but essentially no association of the bacteria with YFP$^+$ cells (Fig. 7; see Movie S5). Experiments with the KIM5 strain yielded similar results (data not shown). We conclude from these experiments that the *Y. pestis* strains used here rarely associate with the YFP$^+$ cells in the dermis of this DC reporter mouse strain, suggesting that DCs play a much less important role than neutrophils in the early events of i.d. *Y. pestis* infection. These data generated with the attenuated strains support the results of our flow cytometry experiments, in which both the fully virulent and attenuated strains showed minimal interaction with CD11c$^+$ cells *in vivo* (data not shown).

Neither neutrophils nor DCs appear to be essential for *Y. pestis* dissemination from the dermis to the dLN. The flow cytometry and intravital microscopy data showing dynamic interactions between neutrophils and *Y. pestis* led us to hypothesize that neutrophils could play a role in dissemination of the bacteria from the dermis to the dLN. We measured dissemination of the virulent 195/P strain of *Y. pestis* in neutrophil-depleted (RB6 8C5 Ab-treated) or control (isotype control Ab-treated) C57BL/6 mice at 24 hpi. The results show no statistically significant difference in the number of viable bacteria in the dLN between the neutrophil-depleted and replete groups (Fig. 8). To account for the possibility that DCs might be capable of compensating for the near absence of neutrophils, we included a *ccr7*$^{-/-}$ mutant mouse strain in our experiment. The CCR7 molecule is required for normal homing of DCs from peripheral tissues to lymphoid tissue (16). Therefore, one would expect neutrophil-depleted *ccr7*$^{-/-}$ mutant mice to exhibit greatly reduced traffic of neutrophils and DCs to the dLN. Interestingly, the neutrophil-depleted and replete groups of *ccr7*$^{-/-}$ mutant mice did not differ in CFU numbers in the dLN. These results suggest that neither neutrophils nor DCs are essential for dissemination of *Y. pestis* to the dLN.

DISCUSSION

Y. pestis is introduced into the dermis of a mammalian host species via the bite of an infected flea. By approximately 6 to 12 hpi, bacteria have begun to disseminate from the dermis to the dLN,

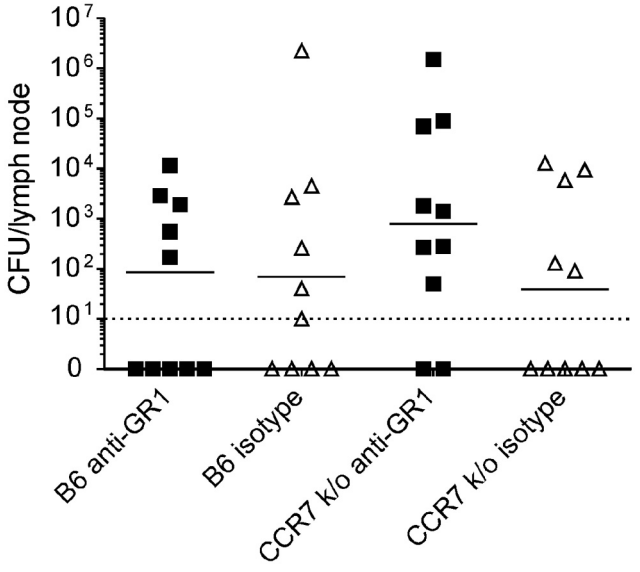

FIG 8 Neutrophil depletion and lack of CCR7-mediated LN homing do not affect the kinetics of *Y. pestis* dissemination. C57BL/6 or *ccr7*$^{-/-}$ mutant mice were injected intraperitoneally with 250 μg of anti-GR1 Ab () or a rat isotype control Ab (Δ) at 24 and 4 h prior to infection. The mice were then infected i.d. with 1,000 CFU in the right hip. At 24 hpi, mice were euthanized and the dLNs (inguinal) were collected. Numbers of CFU in dLNs were determined by plating on blood agar. The dashed line indicates the limit of detection of the assay (10 CFU/lymph node). k/o, knockout.

where they rapidly multiply. Very little is known about the early host cell response to *Y. pestis* in the dermis. We used flow cytometry, confocal microscopy, and several microbiologic techniques to examine early *Y. pestis*-host cell interactions *in vivo*, with a focus on neutrophils and DCs. Additionally, we investigated the potential roles of both neutrophils and DCs in bacterial dissemination from the dermis to the dLN.

The importance of neutrophils in the response to pathogens in the dermis is well established. Neutrophils begin arriving at an i.d. injection site within minutes, even in response to an injection of sterile PBS, showing that trauma or a break in the skin is all that is needed for early neutrophil recruitment (14; J. G. Shannon, unpublished observations). Several studies have examined the importance of neutrophils in bubonic plague pathogenesis. Janssen et al. observed viable *Y. pestis* within neutrophils from the peritonea of infected guinea pigs (17). Sebbane et al. showed that neutrophils are recruited to buboes in rats and *Y. pestis* genes essential for combating neutrophil-derived reactive nitrogen species are highly upregulated *in vivo* (18). *Y. pestis* bacteria taken up by human neutrophils *in vitro* are killed, but a small proportion of the bacteria remain viable and this survival is dependent on a bacterial two-component regulatory system (19, 20). Additionally, pCD1$^+$ strains of *Y. pestis* inhibit the human neutrophil oxidative burst and apoptosis *in vitro* (21). Marketon et al. used a beta-lactamase reporter system to show that neutrophils, along with Mφ and DCs, are injected with *Y. pestis* type III secretion system effectors *in vivo* (22).

We found that >80% of the dsRed$^+$ bacteria in our ear dermis samples were associated with neutrophils at 4 hpi, and this association was not affected by pCD1. Interestingly, only 15 to 30% of the total number of recovered CFU were cell associated at this time point, indicating that there is a population of bacteria that remain extracellular throughout the early phase of infection. A caveat of these experiments is that a large dose of bacteria (1×10^5) was needed to generate consistent, reliable flow cytometry data. Bosio et al. did similar experiments using challenge doses of 500 or 1,000 CFU and observed comparable cellular recruitment to the site of infection (23). However, that study did not examine cell association, so we do not know if reducing the inoculum to a more biologically relevant dose would affect the percentage of cell association. It should also be noted that we were unable to determine if the dsRed fluorescence in these studies was from live or dead bacteria. We have found that heat-killed dsRed$^+$ *Y. pestis* bacteria maintain fluorescence after uptake by neutrophils *in vitro* over the time frame of this study (data not shown).

We also found that *Y. pestis* strains possessing pCD1 had a significant effect on the activation status of neutrophils recruited to the site of infection that had associated with dsRed$^+$ bacteria. This is consistent with a previous report showing decreased neutrophil activation in response to virulent *Y. pestis* compared to a pCD1$^-$ strain (23). Interestingly, infection with the attenuated KIM5/pCD1$^+$ strain inhibited the activation of bacterium-associated neutrophils (dsRed$^+$), but not the entire neutrophil population, as is seen with fully virulent KIM6$^+$/pCD1$^+$ (WT). Furthermore, infection with the KIM6$^+$ *pgm*$^+$ strain resulted in lower levels of neutrophil activation than did infection with *E. coli*. Thus, in addition to the known virulence factors present on pCD1, *Y. pestis* may possess non-pCD1-encoded mechanisms of reducing neutrophil activation *in vivo*. One potential candidate is the ability of *Y. pestis* to produce a nonstimulatory LPS molecule when grown at 37°C (24). We are currently investigating the effects of this LPS modification on the neutrophil response *in vivo*.

Though we observed the majority (>80%) of the cell-associated *Y. pestis* bacteria in the dermis at 4 hpi were associated with neutrophils, most of the remaining bacteria were associated with Mφ. *Y. pestis* survives and replicates in monocytes and Mφ to a much greater extent than in neutrophils (25–27). It has been suggested that ingestion by neutrophils is a dead end for the bacteria and that only *Y. pestis* bacteria that are phagocytosed by Mφ go on to cause disease (4). Our intravital microscopy data, while not quantitative, show that bacteria that do not interact with neutrophils remain stationary at the injection site, whereas neutrophil-associated bacteria traffic away from the site. Thus, it may be possible that a small subset of *Y. pestis* bacteria survives within neutrophils and that these cells contribute to dissemination. It is also possible that all of the neutrophil-associated bacteria are ultimately killed and that only bacteria that remain extracellular go on to disseminate by a heretofore unknown mechanism. Clearly, a more detailed examination of the infected dermis is needed to determine the ultimate fate of neutrophil- and Mφ-associated populations of *Y. pestis* bacteria.

Our intravital microscopy experiments with LysM-eGFP mice revealed qualitative differences in neutrophil recruitment to *Y. pestis* infection versus *E. coli* infection. Many of the neutrophils appeared to arrest their movement and form dense aggregates at the site of *Y. pestis* infection. These aggregates appear similar to the neutrophil swarms observed by Chtanova et al. after *Toxoplasma gondii* infection (28). In contrast, the neutrophils recruited after *E. coli* infection continued to move after contact with bacteria and did not aggregate. We speculate that very different signals are pro-

duced by *Y. pestis*-infected tissue that are not found after infection with the more innocuous bacterium *E. coli* and that these signals may alter the behavior of the recruited neutrophils.

The intravital microscopy experiments described here show a very rapid, localized neutrophil response to *Y. pestis* infection. This is in contrast to our flow cytometric analysis of samples derived from an entire ear that show no significant increase in total neutrophil numbers in the ear at 4 hpi and a previous report showing variable neutrophil numbers in the ear at early time points postinfection (23). This discrepancy highlights the importance of studying the discrete focus of infection *in situ*, as important aspects of pathogenesis can be missed when one analyzes infected tissues as a whole.

DCs are phagocytic antigen-presenting cells that serve as immune sentinels against tissue damage or invasion by potential pathogens. Immature DCs reside in peripheral tissues like the dermis. Upon contact with inflammatory signals, such as microbe-associated ligands of pattern recognition receptors or host-derived molecules associated with tissue damage, DCs undergo a complex maturation process that results in, among many other things, upregulation of the chemokine receptor CCR7 (29). This leads to the migration of DCs along a chemokine gradient out of the peripheral tissues and into the lymphatics, where they can initiate an adaptive immune response. This migration has led to speculation that DCs are responsible for the dissemination of *Y. pestis* bacteria from the dermis to the dLN that occurs in bubonic plague (30, 31); however, minimal data exist to support this hypothesis. Our results suggest that DCs may not play a significant role in the early phase of i.d. *Y. pestis* infection. On the basis of our data that show dynamic interactions between *Y. pestis* and neutrophils *in vivo*, we explored the possibility that neutrophils play a role in dissemination. There is evidence that neutrophils can transport other bacterial pathogens to the dLN (32); however, neutrophil depletion had no effect on *Y. pestis* dissemination in our experiments with a mouse model of bubonic plague. We have been unable to determine the mechanism of this dissemination, and it continues to be a subject of study in our laboratory.

The pCD1 genes encoding known virulence factors are expressed at low levels during growth at the low ambient temperatures experienced while in the flea (33, 34). It is believed that *Y. pestis* requires 3 to 5 h of growth at 37°C to upregulate the pCD1-encoded type III secretion system and secreted effectors (34–36). Interestingly, even though we grew the bacteria at 22°C prior to inoculation to mimic flea transmission, we observed a measurable effect of the virulence plasmid on neutrophil activation at 4 hpi. This suggests that, even at this early time point, the bacteria have produced these virulence factors to a level sufficient for at least partial subversion of the host's normal innate response.

We initiated these studies to elucidate the events that occur in the dermis very early after infection with *Y. pestis*. Our results build upon the established importance of the pCD1 virulence plasmid as a key virulence factor of this pathogen. Additionally, the data presented here highlight the importance of neutrophils in the initial response to i.d. *Y. pestis* infection and indicate that subversion of the normal innate neutrophil response is an important component of bubonic plague pathogenesis.

MATERIALS AND METHODS

Bacterial strains and plasmids. The fully virulent 195/P (37) and KIM6$^+$/pCD1$^+$ (referred to as the WT) strains and the attenuated KIM5 (referred to as pCD1$^+$ and *pgm* locus deficient) and KIM6$^+$ (referred to as pCD1 virulence plasmid deficient and *pgm*$^+$) strains were used in this study. The WT (KIM6$^+$/pCD1$^+$) strain was generated by transformation of KIM6$^+$ with the pCD1 plasmid into which a kanamycin resistance cassette had been inserted as previously described (38). Similarly, this pCD1-kan^r plasmid was transformed into pCD1$^+$ (KIM5). Use of the pCD1-kan^r plasmid allowed the selection of pCD1-containing bacteria by growth in the presence of kanamycin, thus reducing problems associated with loss of pCD1 under certain *in vitro* culture conditions. The *E. coli* strain used was the K-12-derived cloning strain TOP10 (Invitrogen, Carlsbad, CA). All strains were transformed by electroporation with the plasmid pTac-dsRed, which allows the expression of dsRed under the control of an inducible promoter. This pTac-dsRed plasmid was constructed by amplifying the dsRed gene from the pDsRed Express 2 vector (Clontech, Mountain View, CA) by PCR with forward primer 5′ CGCTCGAGTAATGGA TAGCACTGAGAACGTCA 3′ and reverse primer 5′ GCGAATTCGCGG CCGCTACTGGAACA 3′. The PCR product and the vector pTAC-MAT-Tag-2 (Sigma, St. Louis, MO) were digested with XhoI and EcoRI and ligated to form pTac-dsRed.

Bacteria were grown in brain heart infusion (BHI) broth at 28°C with 100 μg/ml carbenicillin to maintain the pTac-dsRed plasmid and 75 μg/ml kanamycin to maintain pCD1-kan^r where appropriate. IPTG (Sigma) was added at a concentration of 100 to 200 μM to induce dsRed expression. Bacterial cultures were transferred to 22°C 12 h prior to infection. Bacteria were washed in PBS, and Lysing Matrix H bead tubes (MP Biomedicals, Solon, OH) and a Fastprep Bio101 (Thermo, Fisher Scientific, Waltham, MA) were used to break up clumps of bacteria in cultures prior to injection. Bacteria were enumerated in a Petroff-Hausser counting chamber before preparation of the inocula in PBS. Serial dilutions of inocula were plated on blood agar to determine the actual number of CFU injected.

We have tested the virulence of the KIM6$^+$/pYV$^+$ strain expressing dsRed in the mouse model of bubonic plague. Mice were challenged i.d. with 100 CFU of this strain. All mice exhibited terminal symptoms and were euthanized between 3.5 and 5 days postinfection, similar to mice challenged with strains lacking the dsRed plasmid (data not shown). All work with the fully virulent KIM6$^+$/pCD1$^+$ strain was performed in a BSL-3 or animal BSL-3 laboratory under a protocol approved by the Rocky Mountain Laboratories Biosafety Committee and in accordance with CDC select agent regulations.

Mice. C57BL/6J LysM-eGFP knock-in mice were originally created by T. Graf (Albert Einstein University, Bronx, NY) (13) and were bred by Taconic Laboratories under a contract with NIAID. C57BL/6J (stock number 000664) and *ccr7*$^{-/-}$ mutant (stock number 006621) mice were purchased from The Jackson Laboratory (Bar Harbor, ME). Ten- To 20-week-old female mice were used in all experiments. All mice were maintained at the Rocky Mountain Laboratories animal care facility under specific-pathogen-free conditions.

Ethics statement. All animal studies were performed under protocols adhering to guidelines established by the American Association for Laboratory Animal Science (AALAS) and the U.S. Public Health Service Office of Laboratory Animal Welfare (PHS-OLAW). The protocols were reviewed and approved by the Rocky Mountain Laboratories Animal Care and Use Committee (AALAS unit number 000462, PHS-OLAW number A-4149-01).

Tissue processing for flow cytometry and microscopy. To evaluate the cell association of *Y. pestis* by flow cytometry, mice were infected i.d. in the ear with 1×10^5 bacteria suspended in 10 μl PBS. At 4 hpi, mice were euthanized and their ears were harvested. Ears that were injected with PBS alone or left unmanipulated and uninjected served as controls. Single-cell suspensions were prepared as described in reference 23, with minor modifications. Briefly, the ventral and dorsal ear dermal layers were separated and incubated for 30 min at 37°C in digestion medium (complete RPMI supplemented with 25 mM HEPES, 1.5 g/liter $NaHCO_3$ [Invitrogen, Carlsbad, CA], 170 μg/ml Liberase [Roche, Indianapolis, IN], and

50 μg/ml deoxyribonuclease I [Worthington Biochemical, Lakewood, NJ]). Following incubation, the dermal tissue was agitated in medium, filtered through a 30-μm nylon strainer, and washed with PBS. The cell suspension was then treated with red blood cell lysis buffer (ammonium-chloride-potassium), and cells were washed with PBS and either pelleted for cytospin and microscopy or resuspended in ice-cold flow cytometry buffer (PBS supplemented with 2% heat-inactivated fetal bovine serum) for staining with fluorescent Abs. The Abs included V450-labeled anti-CD19, PerCP-Cy5.5-labeled anti-CD11c, and Alexa Fluor 488-, 647-, and 700-labeled anti-CD11b, F4/80, and Ly6G (clone 1A8) Abs, respectively. All fluorochrome-conjugated monoclonal Abs were purchased from BD Biosciences (San Jose, CA) or eBioscience (San Diego, CA). All data were collected on an LSRII flow cytometer (Becton Dickinson, San Jose, CA) and analyzed with FlowJo software (Treestar, Ashland, OR). To rule out the possibility that some bacterium-host cell interactions were occurring during the cell isolation and staining procedures, control experiments were performed where bacteria were injected into the ear after the mouse was euthanized. The ear was then processed and stained exactly as described above. The results showed that minimal cell association occurred during the procedure (data not shown). We have also established that cells containing only one dsRed$^+$ bacterium can be reliably detected by flow cytometry (data not shown).

Cells were prepared for confocal microscopy by using a cytospin 4 (Thermo Scientific, Asheville, NC) (1,000 rpm, 4 min), followed by fixation with 2% paraformaldehyde in PBS for 10 min at room temperature. Neutrophils were stained with rat anti-Ly6G Ab (Bio-X-Cell, West Lebanon, NH), followed by a goat anti-rat Alexa Fluor 488 secondary Ab (Invitrogen). Nuclei were stained with 4′,6-diamidino-2-phenylindole (DAPI; Invitrogen). Images were acquired with a Zeiss LSM 510 Meta confocal microscope, and image files were processed by Imaris 6.3.1 software (Bitplane, South Windsor, CT).

***In vitro* polymorphonuclear leukocyte activation assay.** Wells of 24-well tissue culture plates were coated with 20% normal C57BL/6 mouse serum in PBS and incubated for 30 min at 37°C. Bone marrow cells from C57BL/6 mice were then seeded at a density of 5×10^5/well in 500 μl of RPMI medium without phenol red (Invitrogen). Cultures of KIM5 or KIM6$^+$ bacteria were grown overnight at 22°C in BHI medium and then washed and suspended in PBS. Cells were infected at an MOI of 2 or 20 or mock infected with PBS alone and incubated for 4 h at 37°C in 5% CO_2. Cells were then harvested, stained with anti-Ly6G–Alexa Fluor 700 and anti-CD11b–Alexa Fluor 488 Abs, and analyzed by flow cytometry as described above.

Intravital microscopy. Either LysM-eGFP or CD11c-YFP mice were anesthetized with an isoflurane-O_2 mixture provided by nose cone and injected i.d. in the ventral side of the ear with 1×10^3 cells of dsRed-expressing *Y. pestis* (KIM5 or KIM6$^+$) or *E. coli* in 10 μl PBS. The infected mouse was placed on a microscope stage insert containing a coverslip, and its ear was pressed against the coverslip ventral side down and taped in place. The microscope stage was enclosed in an incubated chamber set at 30°C to maintain the normal body temperature of mice. The ear was imaged with a Zeiss LSM 510 Meta confocal microscope, and z-stacks were captured at 2-min intervals. Image files were processed by Imaris 6.3.1 software (Bitplane, South Windsor, CT).

Bacterial dissemination assay. C57BL/6 or *ccr7*$^{-/-}$ mutant mice were injected with 250 μg of either the neutrophil-depleting rat anti-mouse GR1 (clone RB6-8C5; Bio-X-Cell) or rat isotype control (Bio-X-Cell) Ab in 100 μl PBS at 24 and 4 h prior to infection. This strategy leads to the depletion of >95% of the neutrophils from a mouse (see Fig. S2 in the supplemental material). We found that treatment with the RB6 8C5 or isotype control Ab had no effect on the time to development of terminal symptoms in CCR7 knockout or B6 mice after i.d. infection with WT *Y. pestis*. At time zero, mice were injected i.d. in the right hip with 1×10^3 CFU of *Y. pestis* strain 195/P in 25 μl PBS. All mice were euthanized at 24 hpi, and blood, spleen, and dLN (right inguinal) were collected and stored at −80°C. The spleen and dLN tissues were disrupted with Lysing Matrix H bead tubes (MP Biomedicals) and a mini-BeadBeater 1 (BioSpec Products, Bartlesville, OK). The numbers of CFU in the blood and tissue samples were determined by dilution and plating on blood agar plates. All experiments were done in a BSL-3 laboratory in compliance with the CDC select agent regulations.

Cell association assay. Cell association and bacterial recovery assays were done in parallel with the flow cytometry of ear dermis suspensions. Aliquots of 500 μl were taken from the 10-ml total single-cell suspensions described in the tissue-processing section. These aliquots represent the prespin samples. The remaining cell suspensions were then stained for flow cytometry. The staining procedure involves three low-speed centrifugation steps ($500 \times g$, 5 min, 4°C) that remove >95% of the non-cell-associated bacteria (data not shown). After staining and before fixation, the cell pellets are resuspended in 4 ml flow cytometry buffer. Aliquots of 500 μl representing the postspin samples were then taken. The prespin and postspin samples were disrupted with Lysing Matrix H bead tubes, diluted, and plated to determine the number of CFU present in each sample. The total number of CFU recovered from the ear as a percentage of the inoculum and the percentage of cell-associated CFU were then calculated.

Statistics. Data from experiments measuring levels of CD11b expression on Ly6G$^+$ populations or measuring CFU cell association and bacterial recovery were analyzed by one-way analysis of variance with Tukey's multiple-comparison posttest. Data from the bacterial dissemination assay were analyzed by the Kruskal-Wallis nonparametric test with Dunn's multiple-comparison posttest. All data were analyzed and graphed by Prism5 software (GraphPad Software, San Diego, CA).

SUPPLEMENTAL MATERIAL

Supplemental material for this article may be found at http://mbio.asm.org/lookup/suppl/doi:10.1128/mBio.00170-13/-/DCSupplemental.

Movie S1, MOV file, 9.7 MB.
Movie S1R, MOV file, 1.8 MB.
Movie S2, MOV file, 9.7 MB.
Movie S2R, MOV file, 2.1 MB.
Movie S3, MOV file, 4.4 MB.
Movie S3R, MOV file, 2.2 MB.
Movie S4, MOV file, 7.5 MB.
Movie S5, MOV file, 3.6 MB.
Figure S1, TIFF file, 12.2 MB.
Figure S2, TIFF file, 0.1 MB.

ACKNOWLEDGMENTS

We thank Chris Bosio, Scott Kobayashi, Shelly Robertson, and Justin Spinner for critical review of the manuscript; Anita Mora for technical assistance with figures; and Michael Fay for review of our statistical analyses.

This work was supported by the Intramural Research Program of the National Institute of Allergy and Infectious Diseases, National Institutes of Health.

REFERENCES

1. **Comer JE, Sturdevant DE, Carmody AB, Virtaneva K, Gardner D, Long D, Rosenke R, Porcella SF, Hinnebusch BJ.** 2010. Transcriptomic and innate immune responses to *Yersinia pestis* in the lymph node during bubonic plague. Infect. Immun. **78:**5086–5098.
2. **Sebbane F, Gardner D, Long D, Gowen BB, Hinnebusch BJ.** 2005. Kinetics of disease progression and host response in a rat model of bubonic plague. Am. J. Pathol. **166:**1427–1439.
3. **Lukaszewski RA, Kenny DJ, Taylor R, Rees DG, Hartley MG, Oyston PC.** 2005. Pathogenesis of *Yersinia pestis* infection in BALB/c mice: effects on host macrophages and neutrophils. Infect. Immun. **73:**7142–7150.
4. **Pujol C, Bliska JB.** 2005. Turning *Yersinia* pathogenesis outside in: subversion of macrophage function by intracellular yersiniae. Clin. Immunol. **114:**216–226.
5. **Viboud GI, Bliska JB.** 2005. *Yersinia* outer proteins: role in modulation of

host cell signaling responses and pathogenesis. Annu. Rev. Microbiol. **59:** 69–89.
6. **Fetherston JD, Kirillina O, Bobrov AG, Paulley JT, Perry RD.** 2010. The yersiniabactin transport system is critical for the pathogenesis of bubonic and pneumonic plague. Infect. Immun. **78:**2045–2052.
7. **Hinnebusch BJ, Perry RD, Schwan TG.** 1996. Role of the *Yersinia pestis* hemin storage (*hms*) locus in the transmission of plague by fleas. Science **273:**367–370.
8. **Pujol C, Grabenstein JP, Perry RD, Bliska JB.** 2005. Replication of *Yersinia pestis* in interferon gamma-activated macrophages requires *ripA*, a gene encoded in the pigmentation locus. Proc. Natl. Acad. Sci. U. S. A. **102:**12909–12914.
9. **Une T, Brubaker RR.** 1984. *In vivo* comparison of avirulent Vwa$^-$ and Pgm$^-$ or Pstr phenotypes of yersiniae. Infect. Immun. **43:**895–900.
10. **Lorange EA, Race BL, Sebbane F, Joseph Hinnebusch B.** 2005. Poor vector competence of fleas and the evolution of hypervirulence in *Yersinia pestis*. J. Infect. Dis. **191:**1907–1912.
11. **Mayadas TN, Cullere X.** 2005. Neutrophil beta2 integrins: moderators of life or death decisions. Trends Immunol. **26:**388–395.
12. **Sengeløv H, Kjeldsen L, Diamond MS, Springer TA, Borregaard N.** 1993. Subcellular localization and dynamics of Mac-1 (alpha m beta 2) in human neutrophils. J. Clin. Invest. **92:**1467–1476.
13. **Faust N, Varas F, Kelly LM, Heck S, Graf T.** 2000. Insertion of enhanced green fluorescent protein into the lysozyme gene creates mice with green fluorescent granulocytes and macrophages. Blood **96:**719–726.
14. **Peters NC, Egen JG, Secundino N, Debrabant A, Kimblin N, Kamhawi S, Lawyer P, Fay MP, Germain RN, Sacks D.** 2008. *In vivo* imaging reveals an essential role for neutrophils in leishmaniasis transmitted by sand flies. Science **321:**970–974.
15. **Lindquist RL, Shakhar G, Dudziak D, Wardemann H, Eisenreich T, Dustin ML, Nussenzweig MC.** 2004. Visualizing dendritic cell networks *in vivo*. Nat. Immunol. **5:**1243–1250.
16. **Förster R, Braun A, Worbs T.** 2012. Lymph node homing of T cells and dendritic cells via afferent lymphatics. Trends Immunol. **33:**271–280.
17. **Janssen WA, Surgalla MJ.** 1969. Plague bacillus: survival within host phagocytes. Science **163:**950–952.
18. **Sebbane F, Lemaître N, Sturdevant DE, Rebeil R, Virtaneva K, Porcella SF, Hinnebusch BJ.** 2006. Adaptive response of *Yersinia pestis* to extracellular effectors of innate immunity during bubonic plague. Proc. Natl. Acad. Sci. U. S. A. **103:**11766–11771.
19. **Spinner JL, Cundiff JA, Kobayashi SD.** 2008. *Yersinia pestis* type III secretion system-dependent inhibition of human polymorphonuclear leukocyte function. Infect. Immun. **76:**3754–3760.
20. **O'Loughlin JL, Spinner JL, Minnich SA, Kobayashi SD.** 2010. *Yersinia pestis* two-component gene regulatory systems promote survival in human neutrophils. Infect. Immun. **78:**773–782.
21. **Spinner JL, Seo KS, O'Loughlin JL, Cundiff JA, Minnich SA, Bohach GA, Kobayashi SD.** 2010. Neutrophils are resistant to *Yersinia* YopJ/P-induced apoptosis and are protected from ROS-mediated cell death by the type III secretion system. PLoS One **5:**e9279. doi:10.1371/journal.pone.0009279.
22. **Marketon MM, DePaolo RW, DeBord KL, Jabri B, Schneewind O.** 2005. Plague bacteria target immune cells during infection. Science **309:** 1739–1741.
23. **Bosio CF, Jarrett CO, Gardner D, Hinnebusch BJ.** 2012. Kinetics of the innate immune response to *Yersinia pestis* after intradermal infection in a mouse model. Infect. Immun. **80:**4034–4045.
24. **Rebeil R, Ernst RK, Gowen BB, Miller SI, Hinnebusch BJ.** 2004. Variation in lipid A structure in the pathogenic yersiniae. Mol. Microbiol. **52:**1363–1373.
25. **Cavanaugh DC, Randall R.** 1959. The role of multiplication of *Pasteurella pestis* in mononuclear phagocytes in the pathogenesis of flea-borne plague. J. Immunol. **83:**348–363.
26. **Straley SC, Harmon PA.** 1984. *Yersinia pestis* grows within phagolysosomes in mouse peritoneal macrophages. Infect. Immun. **45:**655–659.
27. **Straley SC, Harmon PA.** 1984. Growth in mouse peritoneal macrophages of *Yersinia pestis* lacking established virulence determinants. Infect. Immun. **45:**649–654.
28. **Chtanova T, Schaeffer M, Han SJ, van Dooren GG, Nollmann M, Herzmark P, Chan SW, Satija H, Camfield K, Aaron H, Striepen B, Robey EA.** 2008. Dynamics of neutrophil migration in lymph nodes during infection. Immunity **29:**487–496.
29. **Förster R, Davalos-Misslitz AC, Rot A.** 2008. CCR7 and its ligands: balancing immunity and tolerance. Nat. Rev. Immunol. **8:**362–371.
30. **Robinson RT, Khader SA, Locksley RM, Lien E, Smiley ST, Cooper AM.** 2008. *Yersinia pestis* evades TLR4-dependent induction of IL-12(p40)2 by dendritic cells and subsequent cell migration. J. Immunol. **181:** 5560–5567.
31. **Zhang SS, Park CG, Zhang P, Bartra SS, Plano GV, Klena JD, Skurnik M, Hinnebusch BJ, Chen T.** 2008. Plasminogen activator pla of *Yersinia pestis* utilizes murine DEC-205 (CD205) as a receptor to promote dissemination. J. Biol. Chem. **283:**31511–31521.
32. **Abadie V, Badell E, Douillard P, Ensergueix D, Leenen PJ, Tanguy M, Fiette L, Saeland S, Gicquel B, Winter N.** 2005. Neutrophils rapidly migrate via lymphatics after *Mycobacterium bovis* BCG intradermal vaccination and shuttle live bacilli to the draining lymph nodes. Blood **106:** 1843–1850.
33. **Bacot AW, Martin CJ.** 1914. Observations on the mechanism of the transmission of plague by fleas. J. Hyg. **3:**423–439.
34. **Cornelis GR, Wolf-xWatz H.** 1997. The *Yersinia* Yop virulon: a bacterial system for subverting eukaryotic cells. Mol. Microbiol. **23:**861–867.
35. **Burrows TW.** 1956. An antigen determining virulence in *Pasteurella pestis*. Nature **177:**426–427.
36. **Burrows TW, Bacon GA.** 1956. The basis of virulence in *Pasteurella pestis*: the development of resistance to phagocytosis *in vitro*. Br. J. Exp. Pathol. **37:**286–299.
37. **Chen TH, Foster LE, Meyer KF.** 1961. Experimental comparison of the immunogenicity of antigens in the residue of ultrasonated avirulent *Pasteurella pestis* with a vaccine prepared with killed virulent whole organisms. J. Immunol. **87:**64–71.
38. **Sun YC, Koumoutsi A, Jarrett C, Lawrence K, Gherardini FC, Darby C, Hinnebusch BJ.** 2011. Differential control of *Yersinia pestis* biofilm formation *in vitro* and in the flea vector by two c-di-GMP diguanylate cyclases. PLoS One **6:**e19267. doi:10.1371/journal.pone.0019267.